Eur. Phys. J. D **23**, 81–90 (2003)
DOI: 10.1140/epjd/e2003-00009-9

THE EUROPEAN PHYSICAL JOURNAL D

Theoretical total ionization cross-sections of CH_x, CF_x, SiH_x, SiF_x ($x = 1-4$) and CCl_4 targets by electron impact

K.N. Joshipura[1,a], M. Vinodkumar[2], B.K. Antony[1], and N.J. Mason[3]

[1] Dept. of Physics, Sardar Patel University, Vallabh Vidyanagar − 388120, India
[2] V P & R P T P Science College, Vallabh Vidyanagar − 388120, India
[3] Dept. of Physics and Astronomy, The Open University, Walton Hall, Milton Keynes, MK7 6AA, UK

Received 23 May 2002 / Received in final form 24 October 2002
Published online 21 January 2003 –

Abstract. Total ionization cross-sections of electron impact are calculated for the molecular targets CH_x, CF_x, SiH_x, SiF_x ($x = 1-4$) and CCl_4 at incident energies 20–3 000 eV. The calculation is based on Complex Scattering Potential approach, as developed by us recently. This leads to total inelastic cross-sections, from which the total *ionization* cross-sections are extracted by reasonable physical arguments. Extensive comparisons are made here with the previous theoretical and experimental data. The present results are satisfactory except for the CF_x and SiF_x ($x = 1-3$) radicals, for which the experimental data are lower than most of the theories by more than 50%.

PACS. 34.80.Dp Atomic excitation and ionization by electron impact

1 Introduction

Theoretical and experimental studies on ionizing collisions of electrons with various radicals and molecules have remained an important subject of interest since long. Interest in these collisions arises in view of the applications of relevant cross-section data in various pure and applied sciences [1,2]. Electron induced ionization and other processes determine the density and reactivity of low-temperature technological plasmas. In general the electron as well as positron induced processes, including ionization as a dominant inelastic channel at intermediate and high energies, play important roles in plasma-processing, aeronomy and in biological systems. The status of knowledge about electron impact ionization of radicals and molecules has been highlighted in references [1,2]. On the experimental side, the total ionization cross-sections (TICS) $Q_{\rm ion}$ of practically all the targets listed in the title have been measured by Tarnovsky group [3] and by Baiocchi *et al.* [4]. Some of these hydrocarbon and fluorocarbon molecules and radicals have also been investigated by other experimental groups all over the world [5–18]. In the present paper we have included e–CCl_4 ionization for which recent measurements are due to Hudson *et al.* [19]. Recommended data on the $Q_{\rm ion}$ for some of the present targets have been given by Christophorou and Olthoff [20]. On the theoretical front, the electron impact TICS for a wide variety of molecules and radicals have been calculated by the Kim group in their BED–BEB models [21], and by Khare *et al.* [22]. A different approach in this regard, called the DM formalism [2,23,24] makes use of the static target properties like electronic sub-shell radii, binding energies and a dynamic *i.e.* energy dependent function to obtain the shell-wise contribution to $Q_{\rm ion}$. Recently, Huo *et al.* [25] have revised the experimental data of [9,10] on e–CF_x systems, and have also calculated the corresponding theoretical results in their "siBED" model. The total cross-sections of different electron-induced processes including ionization in molecular targets have been nicely reviewed by Karwasz *et al.* [26]. A recent calculation of the differential and integrated cross-sections together with the total inelastic (absorption) cross-sections for CF_x is due to Lee *et al.* [27]. In Table 1 we have summarized the experimental as well as theoretical studies carried out on the electron impact ionization of the present targets. This table also highlights the basic properties of these targets that are employed as inputs to the present calculations.

The transient radicals, due to their high reactivity, pose difficulties in the cross-section measurements, and hence the experimental results need to be supplemented through alternative theoretical models. Besides, none of the previous theories discuss ionization *in relation* to other processes like elastic scattering and other inelastic collisions of electron impact. With these aspects in mind, the present authors have developed an approach based on complex, energy-dependent (optical) scattering potential, $V_{\rm opt} = V_{\rm R} + {\rm i}V_{\rm I}$. A preliminary version of the present

[a] e-mail: knjoshipura@yahoo.com

Table 1. Summary of theoretical and experimental studies on total ionization cross-sections of radicals and molecules.

Target	I (eV) [36]	Bond Length (a_0) [36]	References		
			Theory	Experiment	Energy (eV) up to
CH	10.64	C – H; 2.12		[3]	200
			BEB [21], DM [2]		1000
CH_2	10.34	C – H; 2.04		[3]	200
			BEB [21], DM [2]		1000
				[4]	150
CH_3	9.84	C – H; 2.09		[3], [4]	200, 150
			BEB [21], DM [2]		1000
CH_4	12.51	C – H; 2.05		[3]	200
			BEB [21], [22], DM [2]		1000
				[5], [6]	400, 700
				[7], [8]	500, 600
CF	9.11	C – F; 2.40	[12], [25], [27]	[9], [25]	200
			BEB [21], DM [2]		1000
CF_2	11.42	C – F; 2.52	[12], [25], [27]	[9], [25]	200
			BEB [21], DM [2]		1000
CF_3	8.90	C – F; 2.51	[12], [31], [25], [27]	[10], [25]	200
			BEB [21], DM [2]		1000
CF_4	16.19	C – F; 2.50		[11], [15]	200, 500
			BEB [21], [20], [12], DM [2]	[13]	1000
SiH	7.89	Si – H; 2.87		[14]	200
			BEB [21]		1000
SiH_2	8.92	Si – H; 2.76		[14]	200
			BEB [21]		1000
SiH_3	8.74	Si – H; 2.78		[14]	200
			BEB [21]		1000
SiH_4	11.65	Si – H; 2.80		[15], [5]	200, 400
			BEB [21]		1000
SiF	7.40	Si – F; 3.03		[16]	200
			BEB [21], DM [2]		1000
SiF_2	10.78	Si – F; 3.01		[17]	200
			BEB [21], DM [2]		1000
SiF_3	9.30	Si – F; 2.99		[18]	200
			BEB [21], DM [2]		1000
SiF_4	15.7	Si – F; 2.94	-	-	-
CCl_4	11.47	C – Cl; 3.34	See [19]	[19]	215

approach [28] yielded a reasonable agreement with ionization data on the radicals CH_x, NH_x ($x = 1-3$) and OH. Our theory starts with a complex spherical potential $V_{\rm opt}$, that contains a real part $V_{\rm R}$ comprising static ($V_{\rm st}$), exchange ($V_{\rm ex}$) and polarization ($V_{\rm p}$) terms, as follows

$$V_{\rm R} = V_{\rm st}(r) + V_{\rm ex}(r, E_{\rm i}) + V_{\rm p}(r, E_{\rm i}) \qquad (1)$$

where, $E_{\rm i}$ is the incident energy. The imaginary part in $V_{\rm opt}$, also called the absorption potential $V_{\rm abs}$, accounts for the total loss of scattered flux into all the allowed *electronic* channels of excitation and ionization. Solving the Schrödinger equation with $V_{\rm opt}$ under appropriate boundary conditions, leads us to the total (*complete*) cross-section

$$Q_{\rm T}(E_{\rm i}) = Q_{\rm el}(E_{\rm i}) + Q_{\rm inel}(E_{\rm i}). \qquad (2)$$

Here, the first term is the total elastic cross-section and the second term is the *summed-total inelastic* cross-section. This does not incorporate the non-spherical effects, *e.g.* the dipole rotation, which may be added to $Q_{\rm T}$ as in [28]. The cross-section $Q_{\rm inel}$ can be used to extract the TICS $Q_{\rm ion}$. Our theoretical approach, called the Complex Scattering Potential-*ionization contribution* (CSP-*ic*)

method has been applied recently to obtain reliable results in a variety of cases *e.g.*, Ne and Ne* atoms [29], atomic and molecular halogens [30], O–O_2–O_3–O_4 targets [31] etc.

Now, our aim in this paper is to apply the CSP-*ic* method to yet another set of targets, mainly radicals, in the energy range $E_i = 20-3\,000$ eV. Our approach is discussed briefly in the next section and comparisons of the present results with experimental, theoretical and/or recommended data are discussed in Section 3.

2 Theoretical methodology

The theoretical models and details of calculations in the present CSP-*ic* approach are discussed in our recent papers [28–31]. Briefly, the main task here is to calculate the summed-total inelastic cross-section $Q_{\rm inel}$ from $V_{\rm opt}$, by employing the spherical part of the target-electron charge density $\rho(r)$. Staszewska *et al.* [32] had developed a quasi-free, Pauli-blocking, dynamic absorption potential (in au), as follows

$$\begin{aligned} V_{\rm abs}(r, E_i) &= -\frac{1}{2}\rho(r)\, v_{\rm loc}\, \sigma_{\rm ee} \\ &= -\rho(r) \left(\frac{T_{\rm loc}}{2}\right)^{1/2} \left(\frac{8\pi}{10 k_F^3\, E_i}\right) \\ &\quad \times \theta(p^2 - k_F^2 - 2\Delta)(A_1 + A_2 + A_3). \quad (3) \end{aligned}$$

In these expressions, $v_{\rm loc}$ is the local speed of the external electron, and $\sigma_{\rm ee}$ denotes the average cross-section of the binary collision of the external electron with one of the target electrons. The local kinetic energy of the incident electron is obtained from,

$$T_{\rm loc} = E_i - V_R = E_i - (V_{\rm st} + V_{\rm ex} + V_p). \quad (4)$$

The term V_p *is not significant here. Further*, $p^2 = 2E_i$ in atomic units, $k_F = [3\pi^2\rho(r)]^{1/3}$ is the Fermi wave vector and Δ is an energy parameter. In equation (3), $\theta(x)$ is the Heaviside unit step-function, such that $\theta(x) = 1$ for $x > 0$ and is zero otherwise. The dynamic functions A_1, A_2 and A_3 defined in Staszewska *et al.* [32] depend differently on $\rho(r)$, I, Δ and E_i. The parameter Δ assumed to be fixed in the original model determines a threshold below which $V_{\rm abs} = 0$, and the ionization or excitation is prevented energetically. We have made modifications [30,31] to choose the value of Δ by the following consideration. At energy of impact close to (vertical) ionization threshold I, the excitations to the discrete states also take place, but as E_i increases the valence ionization becomes dominant, together with the possibility of ionization of the inner electronic shells. The inner shells are of course harder to be excited or ionized. This situation is represented by selecting $\Delta \approx I$ for low E_i and $\Delta > I$ at E_i above the position of the peak of $Q_{\rm inel}$. This is effectively done by expressing Δ as a slowly varying function of E_i around I. Thus with a reasonable choice of the Δ parameter for a given target we construct the $V_{\rm abs}$. The Schrödinger equation when solved numerically for $V_{\rm abs}$, yields the imaginary part of the phase shifts $\mathrm{Im}\,\delta_l(k)$ for various partial waves l. We have omitted here the standard formulae used [28–31] to generate $Q_{\rm inel}$ as well as the $Q_{\rm el}$ by employing the real and the imaginary parts of $\delta_l(k)$.

Let us focus on the inelastic cross-section $Q_{\rm inel}$, which is a quantity not accessible directly in experiments. This cross-section can be partitioned basically as follows

$$Q_{\rm inel}(E_i) = \sum Q_{\rm exc}(E_i) + Q_{\rm ion}(E_i). \quad (5)$$

In this break-up, the first term is the sum over total excitation cross-sections for all accessible electronic transitions, while the second term indicates the total cross-section of all allowed ionization processes of the target by the incident electrons. The first term arises mainly from the low-lying dipole allowed transitions for which the cross-sections become small progressively above the ionization threshold. Hence, as the incident energy increases the second term in equation (5) dominates over the first. It follows from equation (5) that,

$$Q_{\rm inel}(E_i) \geq Q_{\rm ion}(E_i). \quad (6)$$

Now, in order to determine $Q_{\rm ion}$ from the calculated $Q_{\rm inel}$ for a given target, let us define the following quantity for $E_i \geq I$

$$R(E_i) = \frac{Q_{\rm ion}(E_i)}{Q_{\rm inel}(E_i)} \quad (7)$$

such that,

$$0 \leq R \lesssim 1.$$

We require that $R = 0$ at $E_i \leq I$. For a number of stable molecules like O_2, H_2O, CH_4, SiH_4 etc., for which the experimental cross-sections $Q_{\rm ion}$ are known accurately [26], the ratio rises steadily as the energy increases above the threshold, and it is found [28–31] that

$$R(E_i) = R_p, \quad \text{at} \quad E_i = E_p \quad (8a)$$

$$\cong 1, \quad \text{for} \quad E_i > E_p \quad (8b)$$

where, E_p stands for the incident energy at which the calculated $Q_{\rm inel}$ attains its maximum. R_p stands for the value of R at $E_i = E_p$, and as per our discussion in [28–31] we choose here $R_p \cong 0.7$. This choice corresponds to the general observation that at energies close to peak of ionization, the contribution of the molecular $Q_{\rm ion}$ is about 70–80% in the total inelastic cross-sections $Q_{\rm inel}$. For the calculation of $Q_{\rm ion}$ from $Q_{\rm inel}$ we need R as a continuous function of energy, hence we represent [31] the ratio R at energies $E_i \geq I$ in the following manner

$$R(E_i) = 1 - f(U),$$

i.e.,

$$R(E_i) = 1 - C_1 \left[\frac{C_2}{U + a} + \frac{\ln(U)}{U}\right]. \quad (9)$$

Here U is the dimensionless variable defined through,

$$U = \frac{E_{\rm i}}{I}. \tag{10}$$

The reason for adopting a particular functional form of $f(U)$ *i.e.* the second term in equation (9) is as follows. As $E_{\rm i}$ increases above I, the ratio R increases from zero and approaches value 1, since the ionization contribution rises and the discrete excitation term in equation (5) decreases. The discrete excitation cross-sections, dominated by dipole transitions, fall off as $\ln(U)/U$ at high energies. Accordingly the decrease of the function $f(U)$ must also be proportional to $\ln(U)/U$ in the high range of energy. However, the two-term representation of $f(U)$ given in equation (9) is more appropriate since the 1st term in the square bracket ensures a better energy dependence at low and intermediate $E_{\rm i}$ [31]. Equation (9) involves dimensionless parameters C_1, C_2 and a that reflect the target properties. To determine these parameters, we note the following three conditions on the ratio R. (i) It is zero at and below the ionization threshold. (ii) It behaves in accordance with equation (8a) at the peak position $E_{\rm p}$, and (iii) it approaches 1 asymptotically for $E_{\rm i}$ sufficiently larger than $E_{\rm p}$. Equations (6–10) define the present CSP-*ic* approach [29–31].

The present method employs two of the most well-known target properties *viz.*, the first ionization energies and the bond lengths, as the basic inputs. Unlike the BEB [21], siBED [25] and the DM [2] approaches of ionization calculations, the present method does not consider shell-wise contribution to the quantity $Q_{\rm ion}$. Rather, the absorption potential $V_{\rm abs}$ employed here to account (mainly) for ionization, sweeps through the region of the charge-cloud continuously, and vanishes in between. At higher incident energies the potential penetrates deeper into the electronic shells, but decreases in strength. The energy range and the Δ parameter chosen presently are such that the present theory describes mainly the valence electron ionization.

Although the focus of this paper is on ionization, the basic method provides the approximate contributions of $Q_{\rm ion}$ as well as $\sum Q_{\rm exc}$ in the total quantity $Q_{\rm inel}$. This can be coupled with $Q_{\rm el}$ to obtain the approximate contributions of all the major total cross-sections at certain energy for a given target, as done in our recent work on O–O_2–O_3–O_4 systems [31]. For the present targets however, not much is known for processes other than ionization.

3 Results and discussion

First of all, let us examine the behaviour of the function R with respect to incident energy $E_{\rm i}$, as expressed in equation (9). This is plotted in Figure 1 for the selected targets CH, CH_4, CF_3 and SiF_3. The approach of R to value 1 depends mainly on the ionization threshold I, and to some extent on the peak position $E_{\rm p}$, as seen from this figure.

Now, our interest here is in the ionization of radicals since in some of them-especially the fluoride radicals-

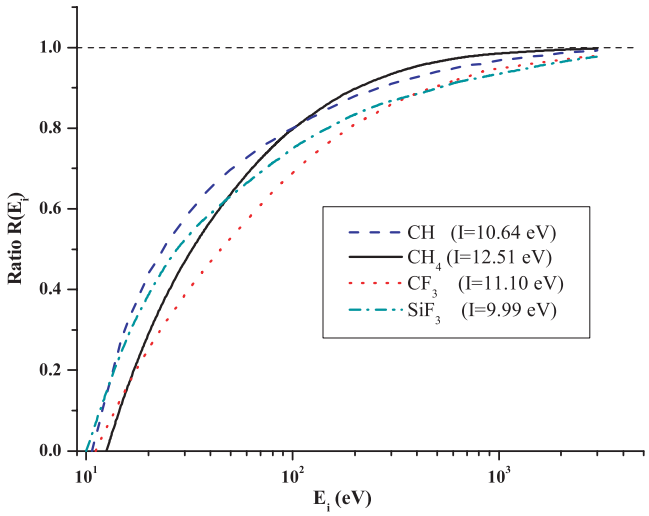

Fig. 1. Ratio $R(E_{\rm i})$ *vs.* $E_{\rm i}$ for various targets, (– – – – –) CH, (———) CH_4, (· · · · ·) CF_3, (–·–·–·–) SiF_3.

there is a big discrepancy between the theoretical (except Ref. [25]) and the experimental data. We have presented our calculations on 17 molecular targets and compared graphically in Figures 2 to 6 the *TICS* $Q_{\rm ion}$ for the molecular species CH_x, CF_x, SiH_x and SiF_x as well as CCl_4, with different sets of previous data. While making comparisons of our values with the experimental TICS, we added together the parent and all the dissociative ionization data as tabulated separately by experimentalists in each case.

CH_x (x = 1−3) and CH_4

The present as well as previous cross-sections $Q_{\rm ion}$ of CH, CH_2 and CH_3 hydrocarbon radicals are exhibited in Figures 2a–2c, while the CH_4 cross-sections are plotted in Figure 2d. For all the three CH_x radicals our present theory yields ionization cross-sections that are in good agreement with the BEB theory of Ali *et al.* [21]. Both these theoretical results, though on the higher side of the experimental data, are within the error limit of 17% in the measurements of [3,4]. In the case of the stable molecule CH_4 (Fig. 2d), the present results are in good accord with other theoretical [21] as well as experimental [5–8] results. The C–H bond lengths in these radicals and in the CH_4 molecule are nearly the same, hence the peak $Q_{\rm ion}$ magnitudes are dependent on the respective ionization potentials. All the reactive radicals AB_x considered in this paper have in common a peculiar property that, their bond lengths A–B are almost similar to that of their parent molecule AB_4, but have the ionization thresholds much *lower* than their parents. Therefore, the relative magnitudes of the present $Q_{\rm ion}$ for the radicals and their parent molecules, appear to be consistent.

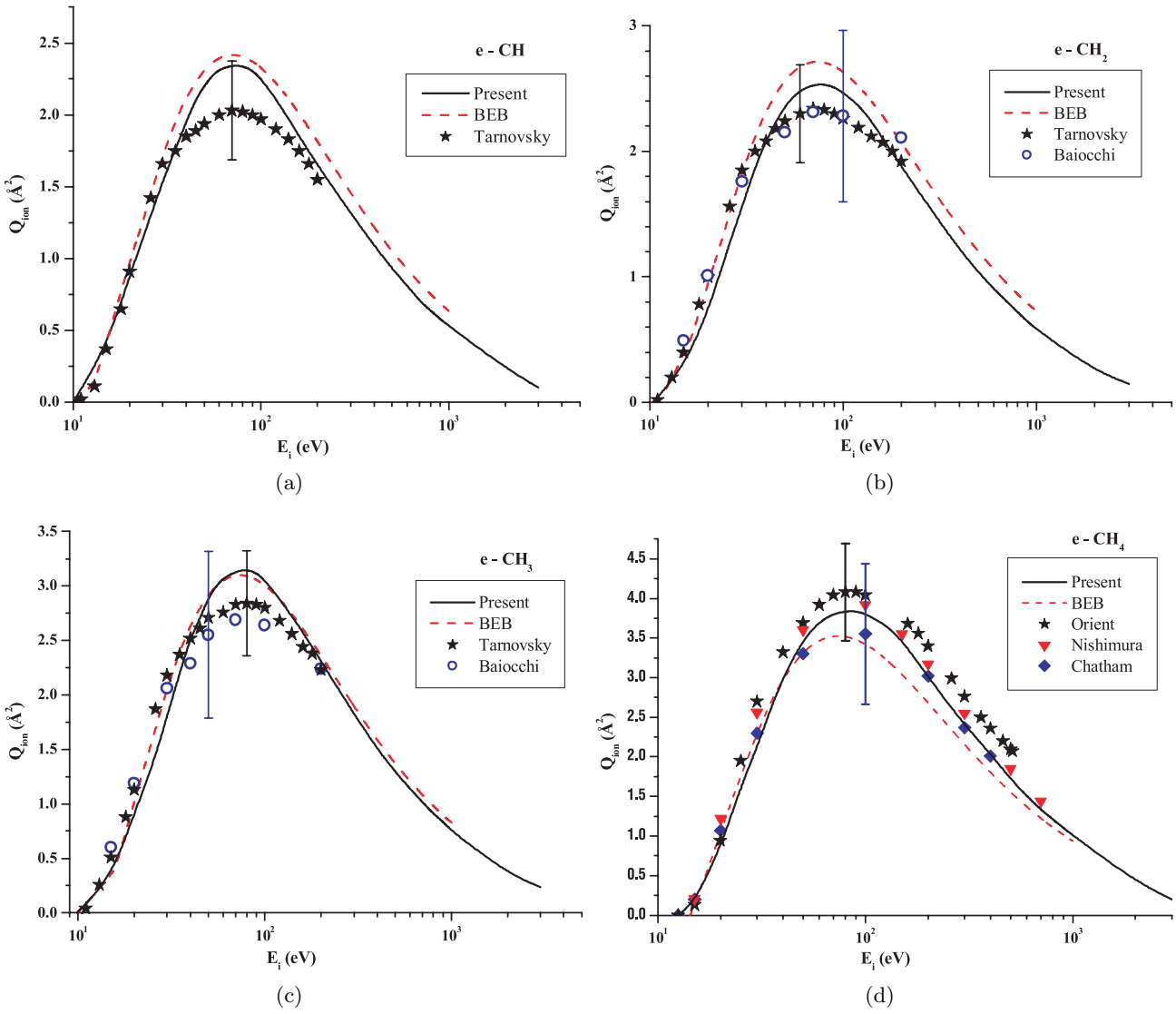

Fig. 2. (a) Total ionization cross-sections for e–CH scattering, (——) present, (– – –) BEB, Ali *et al.* [21], (★★★) Tarnovsky *et al.* [3]. (b) Total ionization cross-sections for e–CH_2 scattering, (——) present, (– – –) BEB, Ali *et al.* [21], (★★★) Tarnovsky *et al.* [3], (○○○) Baiocchi *et al.* [4]. (c) Total ionization cross-sections for e–CH_3 scattering, same as in (b), but for CH_3 radical. (d) Total ionization cross-sections for e–CH_4 scattering, (———) present, (– – –) BEB, Ali *et al.* [21], (★★★) Orient and Srivastava [7], (▼▼▼) Nishimura and Tawara [6], (♦♦♦) Chatham *et al.* [5].

CF_x (x = 1−3) and CF_4

Figures 3a–3c correspond to the fluorocarbon radicals CF, CF_2 and CF_3 respectively, and the comparisons for the ionization cross-section of the parent molecule CF_4 are made in Figure 3d. All the previous theoretical results [2,21] as well as the present one, on the three radicals CF_x are found to be on the higher side of the experimental data (Figs. 3a–3c). We have made comparisons with the recent measurements and calculations on CF, CF_2 and CF_3 by Huo *et al.* [25]. Their experimental results involve an error of 25%. Another calculation on $Q_{\rm inel}$ of these radicals, which is similar to the present work, has been carried out by Lee *et al.* [27]. The results of [27], not shown here, are also on the higher side of [25].

The present and the BEB [21] values exceed the measurements [9,10,25] by more than 50%, while DM calculations [2,23,24] are less higher. Except [25], the theoretical $Q_{\rm ion}$ of CF_3 are comparable to (but not lower than) those of the parent molecule CF_4. This can be attributed to the smaller ionization threshold of the radical, vide Table 1. To preserve clarity in Figure 3c the TICS of CF_3 calculated by Huo *et al.* [25] are not shown, but these are quite close to their own experimental data. Since the results of [25] are distinctly lower than the rest of the data, we have provided a yet another comparison in this figure

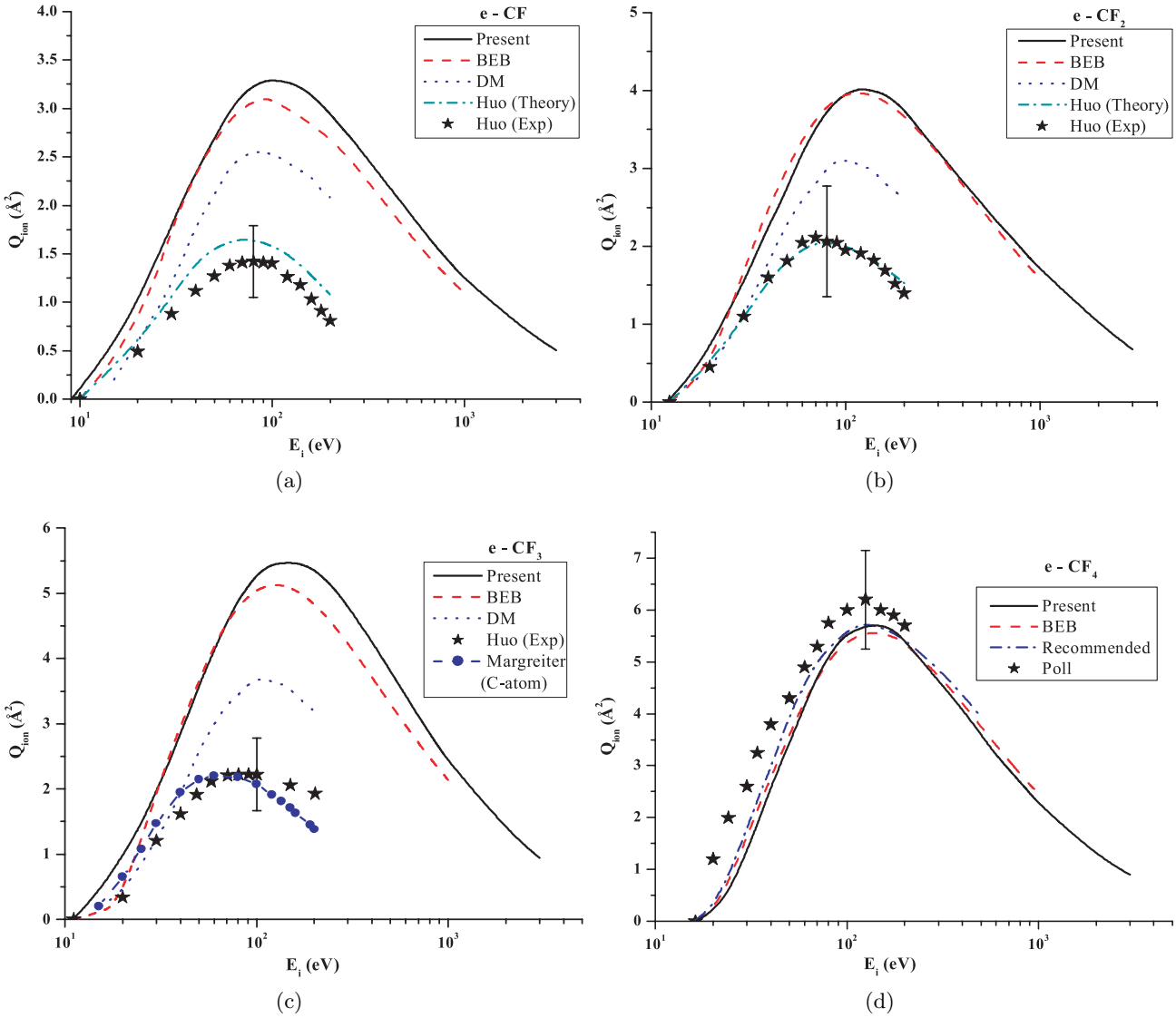

Fig. 3. (a) Total ionization cross-sections for e–CF scattering, (———) present, (– – –) BEB, Ali *et al.* [21], (· · · · ·) DM, Deutsch *et al.* [24], (–·–·–·–) Huo *et al.* (theory) [25], (★★★) Huo *et al.* (Exp.) [25]. (b) Total ionization cross-sections for e–CF_2 scattering, same as (a), but for CF_2 radical. (c) Total ionization cross-sections for e–CF_3 scattering, (———) present, (– – –) BEB, Ali *et al.* [21], (· · · · ·) DM, Deutsch *et al.* [24], (★★★) Huo *et al.* (Exp.) [25], (–●–) C-atom, Margreiter *et al.* [33]. (d) Total ionization cross-sections for e–CF_4 scattering, (———) present, (– – –) BEB, Ali *et al.* [21], (–·–·–·–) recommanded data [20], (★★★) Poll *et al.* [11].

by reproducing the TICS of *the carbon atom* as calculated accurately by Margreiter *et al.* [33]. Notably, the experimental $Q_{\rm ion}$ of CF_3 radical [25] and carbon atom [33] are seen to be nearly equal, at least in the peak region, and this feature remains unexplained.

The theoretical results of Huo *et al.* [25] are based on the "simplified BED (siBED)" model, which considers the screened dipole potential in the original BED model [21]. These authors [25] have replaced the Bethe dipole cross-section of the original model, by the cross-section due to a shielded long range transition dipole potential. Now, in an earlier theoretical work, one of the present authors [34] had shown that the shielding of the pure dipole potential would lead to reduction in the electron impact cross-sections, depending on the extent of the screening itself. In the present context of the siBED model [25] for electron impact ionization problem, however, not only the nature but also the extent of the "screening" is not clear. Further, the TICS of CF_x radicals as obtained in [25] are quite lower than that of the parent molecule CF_4. This behaviour is not understood since the ionization threshold of CF_4 is higher than those of the radicals CF_x.

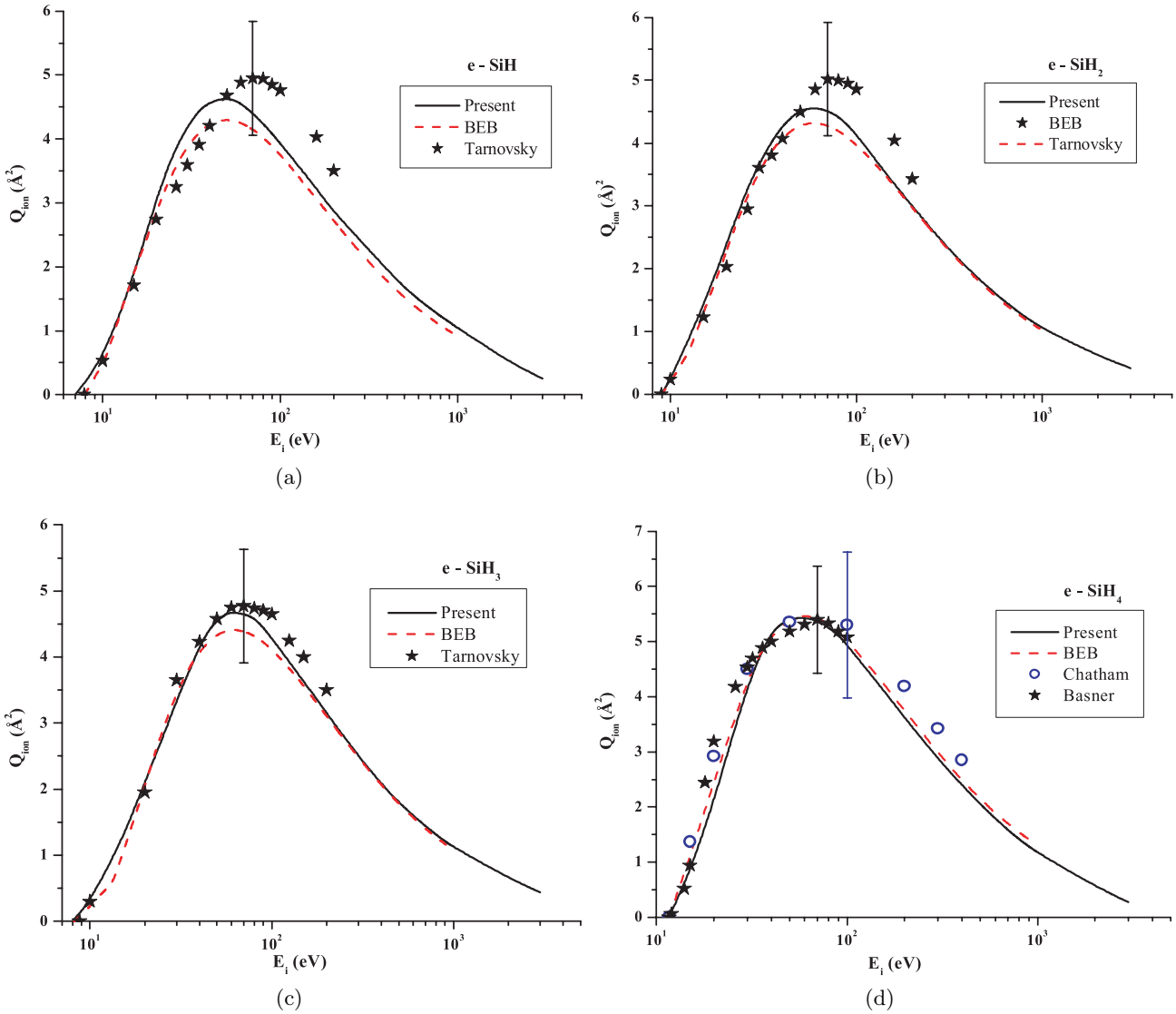

Fig. 4. (a) Total ionization cross-sections for e–SiH scattering, (———) present, (– – –) BEB, Ali *et al.* [21], (★★★) Tarnovsky *et al.* [14]. (b) Total ionization cross-sections for e–SiH_2 scattering, same as (a), but for SiH_2 radical. (c) Total ionization cross-sections for e–SiH_3 scattering, same as (a), but for SiH_3 radical. (d) Total ionization cross-sections for e–SiH_4 scattering, (———) present, (– – –) BEB, Ali *et al.* [21], (○ ○ ○) Chatham *et al.* [5], (★★★) Basner *et al.* [15].

In the case of CF_4 molecule (Fig. 3d) we find a good agreement of the present results with almost all the previous data sets, and in particular with the recommended data of Christophorou and Olthoff [20].

SiH_x ($x = 1-3$) and SiH_4

As shown in Figures 4a–4c, the cross-sections $Q_{\rm ion}$ for the three hydrosilicon radicals SiH_x, calculated in the present CSP-*ic* approach are in a good accord with the BEB model of the Kim group [21] as well as the only available experimental results [14]. We must note here that, the BEB model in this species of radicals was modified to "BEB/3" model [21], wherein the theoretically available kinetic energy of the valence electrons was altered by these authors [21] in order to obtain reliable values of $Q_{\rm ion}$. No such adjustment was needed in the present calculations. Presently we find that the peak positions and the magnitudes of our calculated TICS are in keeping with the ionization thresholds and the number of electrons of the radicals SiH_x ($x = 1-3$).

The present calculations for the parent silane molecule (Fig. 4d) are in a very nice agreement with the previous theoretical [21] and experimental [5,15] data.

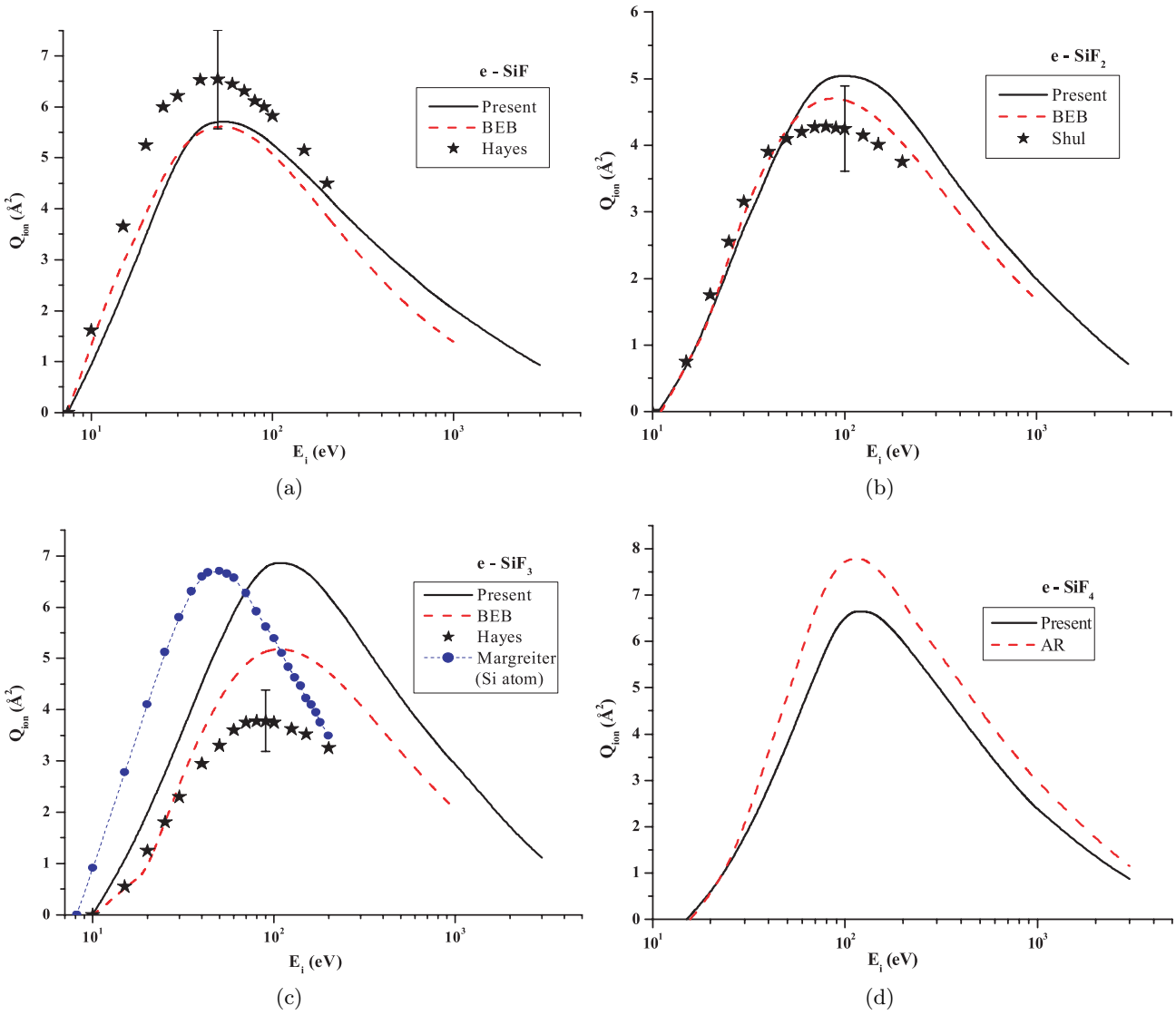

Fig. 5. (a) Total ionization cross-sections for e–SiF scattering, (———) present, (– – –) BEB, Ali *et al.* [21], (★★★) Hayes *et al.* [16]. (b) Total ionization cross-sections for e–SiF_2 scattering, (———) present, (– – –) BEB, Ali *et al.* [21], (★★★) Shul *et al.* [17]. (c) Total ionization cross-sections for e–SiF_3 scattering, (———) present, (– – –) BEB, Ali *et al.* [21], (★★★) Hayes *et al.* [18], (–●–) Si-atom, Margreiter *et al.* [33]; (d) total ionization cross-section for e–SiF_4 scattering, (———) present, (– – –) AR (see text).

The relative magnitudes of the $Q_{\rm ion}$ in the sequence SiH–SiH_2–SiH_3–SiH_4 are understood in terms of their respective properties (Tab. 1).

SiF_x (x = 1−3) and SiF_4

A comparison of the $Q_{\rm ion}$ of the fluorosilicon radicals SiF_x is provided by Figures 5a–5c and Figure 5d shows the present and the previous data sets for SiF_4. As compared to the measurements [16–18], the theoretical data [21] for these radicals lie on the higher side except for SiF (Fig. 5a), and the present values are still somewhat higher than the rest of the theories. This situation is similar to radicals CF_x (Figs. 2a–2c). The discrepancy is maximum in the case of SiF_3 (Fig. 5c). The TICS of *silicon atom* [33] are also exhibited for comparison in that figure. It is interesting to note that, the cross-sections of e–Si *atomic* ionization calculated by [33] and shown in Figure 5c are *higher* than the experimental data [18] on the radical SiF_3. This particular feature is similar to the case of CF_x radicals and is not understood clearly. The e–Si ionization curve is peaking at lower $E_{\rm i}$ due to the lower ionization threshold of the Si atom.

Figure 5d exhibits our present calculations on SiF_4 molecule, in which case there seems to be no previous

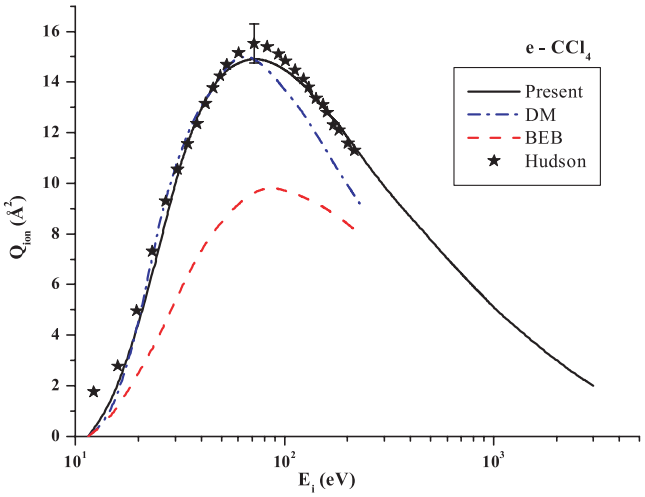

Fig. 6. Total ionization cross-sections for e–CCl_4 scattering, (———) present, (– – –) BEB, Kim (as in Ref. [19]), (–·–·–) DM, Deutsch *et al.* [24], (★★★) Hudson *et al.* [19].

comparative data. We have, therefore, supplemented the present calculations for SiF_4 with an "additivity" [28] calculation. However, it is not appropriate to simply add the $Q_{\rm ion}$ of the constituent atoms in this molecule, in view of a large difference in the ionization thresholds of the Si atom ($I = 8.15$ eV) and the SiF_4 target ($I = 15.7$ eV). Hence, we have considered a fictitious Si atom with $I = 15.7$ eV to be in the SiF_4 target, and simply added the contribution of the four F atoms. As Figure 5d shows, these two calculations made by us produce almost the same shape of the $Q_{\rm ion}$ curve, and the additivity rule (AR) as employed here is on the higher side, as expected.

e–CCl_4 ionization

Finally as shown in Figure 6, our calculated results on the ionization of CCl_4 molecule are in a very good agreement with the recent measurements of the Harland group [19] at all energies. The DM calculations of Margreiter *et al.* [35] on CCl_4 are closer to the present data and the measurements only up to the peak position, after which the DM results tend to be lower. This behaviour was also observed by the present authors in the halogens Br_2 and I_2 [30]. The BEB values on CCl_4 as included in Figure 6 are actually taken from reference [19]. It has been noted by Hudson *et al.* [19] that the BEB results in the case of heavier targets are on the lower side.

4 Conclusions

The recently developed CSP-*ic* method [31] has been applied in this work to calculate total ionization cross-sections for electron impact on various radicals and their parent stable molecules. By and large, the present theoretical results on the stable molecular fluorides and hydrides of the type AB_4 show a satisfactory accord with the numerous other investigations including the recommended data. For the transient radicals since the ionization threshold is lower, the peak $Q_{\rm ion}$ are found to be higher and they occur at relatively lower energies as compared to the parent stable molecules. Practically all the theories, including our own, are seen to overestimate the experimental $Q_{\rm ion}$ values in the case of the reactive *radicals* CF_x and SiF_x ($x = 1-3$). The discrepancy between the present results and the measured data is very high (>50%) in CF_3 and SiF_3 radicals. At the peak positions, the measured data for these radicals are just close to or even less than atomic carbon and silicon cross-sections respectively. The situation here is similar to the difference between theories and experiments in the case of e–F_2 ionization, as examined in our group [30]. The siBED model [25] proposed recently agrees well with the measured data on CF_3 radical, but needs theoretical justification. In the case of all hydrides CH_x and SiH_x ($x = 1-4$), the agreement of the present theory with the previous measurements and theories is found to be quite satisfactory. There is also a good accord between our calculations and recent measurements on e–CCl_4 ionization. The present method provides a reasonable estimate of ionization in relation to electronic excitations in a target. It would be interesting now to apply the CSP-*ic* method to the ionization of other heavier targets.

KNJ thanks the Department of Science & Technology, New Delhi-India for a Research Project under which, a part of this work was carried out.

References

1. N.J. Mason, J.M. Gingell, N.C. Jones, L. Kaminski, Phil. Trans. R. Soc. Lond. A **357**, 1175 (1999)
2. H. Deutsch, K. Becker, S. Matt, T.D. Maerk, Int. J. Mass Spectrom **197**, 37 (2000), and references therein
3. V. Tarnovsky, A. Levin, H. Deustch, K. Becker, J. Phys. B: At. Mol. Opt. Phys. **29**, 139 (1996)
4. F.A. Baiocchi, R.C. Wetzel, R.S. Freund, Phys. Rev. Lett. **53**, 771 (1984)
5. H. Chatham, D. Hils, R. Robertson, A. Gallagher, J. Chem. Phys. **81**, 1770 (1984)
6. H. Nishimura, H. Tawara, J. Phys. B **27**, 2063 (1994)
7. O.J. Orient, S.K. Srivastava, J. Phys. B: At. Mol. Opt. Phys. **20**, 3923 (1987)
8. C. Tian, C.R. Vidal, J. Phys. B: At. Mol. Opt. Phys. **31**, 895 (1998)
9. V. Tarnovsky, P. Kurunczi, D. Rogozhnikov, K. Becker, Int. J. Mass Spectrom. Ion Proc. **128**, 181 (1993)
10. V. Tarnovsky, K. Becker, J. Chem. Phys. **98**, 7686 (1993)
11. H.U. Poll, C. Winkler, D. Margreiter, V. Grill, T.D. Maerk, Int. J. Mass Spectrom. Ion Proc. **112**, 1 (1992)
12. H. Nishimura, W.M. Huo, M.A. Ali, Y.-K. Kim, J. Chem. Phys. **110**, 3811 (1999)
13. D.R. Sieglaff, R. Rejoub, B.G. Lindsay, R.F. Stebbings, J. Phys. B: At. Mol. Opt. Phys. **34**, 799 (2001)
14. V. Tarnovsky, H. Deustch, K. Becker, J. Chem. Phys. **105**, 6315 (1996)

15. R. Basner, M. Schmidt, V. Tarnovsky, K. Becker, Int. J. Mass Spectrom. Ion Proc. **171**, 83 (1997)
16. T.R. Hayes, R.C. Wetzel, F.A. Baiocchi, R.S. Freund, J. Chem. Phys. **88**, 823 (1988)
17. R.J. Shul, T.R. Hayes, R.C. Wetzel, F.A. Baiocchi, R.S. Freund, J. Chem. Phys. **89**, 4042 (1988)
18. T.R. Hayes, R.J. Shul, F.A. Baiocchi, R.C. Wetzel, R.S. Freund, J. Chem. Phys. **89**, 4035 (1988)
19. J.E. Hudson, C. Vallance, M. Bart, P.W. Harland, J. Phys. B: At. Mol. Opt. Phys. **34**, 3025 (2001)
20. L.G. Christophorou, J.K. Olthoff, J. Phys. Chem. Ref. Data **28**, 967 (1999)
21. M.A. Ali, Y.-K. Kim, W. Hwang, N.M. Weinberger, M.E. Rudd, J. Chem Phys. **106**, 9602 (1997); see also their website, `http://physics.nist.gov/PhysRefData/Ionization`
22. S.P. Khare, M.K. Sharma, S. Tomar, J. Phys. B: At. Mol. Opt. Phys. **32**, 3147 (1999)
23. D. Margreiter, H. Deutsch, M. Schmidt, T.D. Maerk, Int. J. Mass Spectrom. Ion Proc. **100**, 157 (1990)
24. H. Deutsch, C. Cornelissen, L. Cespiva, V. Bonacic-Koutecky, D. Margreiter, T.D. Märk, Int. J. Mass Spectrom. Ion Proc. **129**, 43 (1993), and references therein
25. W.M. Huo, V. Tarnovsky, K.H. Becker, Chem. Phys. Lett. **358**, 328 (2002)
26. G.P. Karwasz, R.S. Brusa, A. Zecca, Riv. Nuovo Cim. **24**, 1 (2002)
27. M.-T. Lee, I. Iga, L.M. Brescansin, L.E. Machado, F.B.C. Machado, Phys. Rev. A **66**, 012720 (2002)
28. K.N. Joshipura, V. Minaxi, U.M. Patel, J. Phys. B: At. Mol. Opt. Phys. **34**, 509 (2001)
29. K.N. Joshipura, B.K. Antony, Phys. Lett. A **289**, 323 (2001)
30. K.N. Joshipura, C.G. Limbachiya, Int. J. Mass Spectrom. **216**, 239 (2002)
31. K.N. Joshipura, B.K. Antony, V. Minaxi, J. Phys. B: At. Mol. Opt. Phys. **35**, 4211 (2002)
32. D. Staszewska, D.W. Schwenke, D. Thirumalai, D.G. Truhlar, Phys. Rev. A **29**, 3078 (1984)
33. D. Margreiter, H. Deutsch, T.D. Maerk, Int. J. Mass Spectrom. Ion Proc. **139**, 127 (1994)
34. K.N. Joshipura, S. Mohanan, Z. Phys. D **15**, 67 (1990)
35. D. Margreiter, H. Deutsch, T.D. Maerk, Contrib. Plasma Phys. **30**, 487 (1990); H. Deutsch, K. Becker, T.D. Maerk, Int. J. Mass Spectrom. Ion Proc. **167/168**, 503 (1997)
36. *CRC Handbook Of Physics and Chemistry*, edited by D.R. Lide (Boca Raton FL. USA, 2000), pp. 9–42